

University of Oklahoma for providing computer time.

Registry No. $[(\text{CH}_3)_2\text{SnCl}_2\text{O}=\text{CC}_2(\text{C}_6\text{H}_5)_2]_2$, 82639-34-7.

Supplementary Material Available: A listing of observed and calculated structure amplitudes, the thermal parameters (Table

IV), hydrogen parameters (Table VII), the carbon-carbon and carbon-hydrogen distances and the carbon-carbon-carbon angles in the phenyl rings (Table VIII), and least-squares planes (Table IX) (24 pages). Ordering information is given on any current masthead page.

Polarized X-ray Absorption Spectra of Oriented Plastocyanin Single Crystals. Investigation of Methionine-Copper Coordination

Robert A. Scott,^{†,‡} James E. Hahn,[‡] Sebastian Doniach,[§] Hans C. Freeman,^{*||} and Keith O. Hodgson^{*†}

Contribution from the Departments of Chemistry and Applied Physics, Stanford University, Stanford, California 94305, and the Department of Inorganic Chemistry, University of Sydney, N.S.W. 2006, Australia. Received January 4, 1982

Abstract: Polarized X-ray absorption spectra have been recorded for oriented single crystals of the "blue" copper protein plastocyanin from *Populus nigra* var. *italica*. From the crystal structure of plastocyanin, it is known that the sulfur atom of a methionine residue is located 2.90 Å from the Cu atom. In prior analyses of the extended X-ray absorption fine-structure (EXAFS) spectra of plastocyanin and other blue copper proteins in solution, the contribution of this sulfur to the EXAFS appeared to be weak or absent. The symmetry properties of plastocyanin crystals have now enabled us to record X-ray absorption spectra of plastocyanin in two orientations in which all of the Cu-S(Met) bonds are either parallel to or perpendicular to the polarization vector of the incident synchrotron X-radiation. In the first of these orientations, the ability to detect the Cu-S(Met) EXAFS should be significantly enhanced. Comparison of spectra from the two orientations confirms that the methionine sulfur makes a negligible contribution to the EXAFS. Possible reasons for this noncontribution, and their significance for EXAFS structure determinations, are discussed. In addition, the structure of the X-ray absorption edge of plastocyanin crystals is found to be strongly orientation dependent.

The so-called "type 1" or "blue" copper proteins have an extremely intense (ca. 3000–5000 M⁻¹ cm⁻¹) absorption band near 600 nm, a very small hyperfine splitting in the g_{\parallel} region of the EPR spectrum, and an unusually high reduction potential. A great deal of effort has been devoted to developing a detailed structural interpretation of these unique features. The molecular structures of two blue copper proteins, plastocyanin from poplar leaves (*Populus nigra* var. *italica*) and azurin from *Pseudomonas aeruginosa*, are now known from X-ray crystallographic studies.^{1,2} In the oxidized [Cu(II)] state, both proteins contain a copper atom coordinated to the nitrogen atoms of two histidine residues, a cysteine sulfur, and a methionine sulfur. A refinement of the plastocyanin structure at 1.6-Å resolution has shown that the metal-ligand distances are Cu-N(His) = 2.04 and 2.10 Å, Cu-S(Cys) = 2.13 Å, and Cu-S(Met) = 2.90 Å, with esd's of about 0.05 Å.^{3,4} Although the unique features of blue copper protein sites have been substantially rationalized in terms of the X-ray structural results, the significance of the extremely long Cu-S(Met) bond in relation to the properties of plastocyanin remains a subject for speculation and study.^{4,5} Single-crystal electronic absorption spectra and EPR spectra have shown that the methionine sulfur has at most a very small effect on the ligand field at the copper atom.⁶

Previous extended X-ray absorption fine-structure (EXAFS) analysis of solutions of plastocyanin from French beans (*Phaseolus vulgaris*) yielded results in substantial agreement with the crystallographic distances from the copper to the three close ligands (2 N(His) at 1.97 Å and an S(Cys) at 2.11 Å).⁷ However, as

in similar experiments on solutions of azurin,⁸ the presence of the more distant S(Met) ligand could not be unequivocally demonstrated from the EXAFS analysis. In order to improve our understanding of the contribution of the S(Met) ligand to the Cu EXAFS, we have undertaken an X-ray absorption spectroscopic study of plastocyanin single crystals. To the best of our knowledge, this is the first such study of a protein in the crystalline state.

Plastocyanin crystallizes in the orthorhombic space group $P2_12_12_1$ with four molecules per unit cell. These four symmetry-related molecules have their Cu-S(Met) bonds aligned approximately parallel to the crystallographic c axis. The three other copper-ligand bonds in each molecule lie roughly normal to the c axis as a result of the distorted tetrahedral (or elongated C_{3v}) coordination geometry of the Cu atoms. These symmetry properties are crucial to the experiments described herein.

The amplitude of the EXAFS from a given scatterer is proportional to the square of the cosine of the angle between the X-ray

(1) Colman, P. M.; Freeman, H. C.; Guss, J. M.; Murata, M.; Norris, V. A.; Ramshaw, J. A. M.; Venkatappa, M. P. *Nature (London)* **1978**, *272*, 319-324.

(2) Adman, E. T.; Stenkamp, R. E.; Sieker, L. C.; Jensen, L. H. *J. Mol. Biol.* **1978**, *123*, 35-47. Adman, E. T.; Jensen, L. H. *Isr. J. Chem.* **1981**, *21*, 8-12.

(3) Guss, J. M.; Freeman, H. C., unpublished work. We draw attention to an unfortunate typographical error in ref 6 where the copper-ligand bond length esd's in plastocyanin are cited as 0.02 Å.

(4) Freeman, H. C. In "Coordination Chemistry-21"; Laurent, J. P., Ed.; Pergamon Press: Oxford, 1981; pp 29-51.

(5) Dagdigan, J. V.; McKee, V.; Reed, C. A. *Inorg. Chem.* **1982**, *21*, 1332-1342.

(6) Penfield, K. W.; Gay, R. R.; Himmelwright, R. S.; Eickman, N. C.; Norris, V. A.; Freeman, H. C.; Solomon, E. I. *J. Am. Chem. Soc.* **1981**, *103*, 4382-4388.

(7) Tullius, T. D. Ph.D. Thesis, Stanford University, 1979.

(8) Tullius, T. D.; Frank, P.; Hodgson, K. O. *Proc. Natl. Acad. Sci. U.S.A.* **1978**, *75*, 4069-4073.

[†] Present address: School of Chemical Sciences, University of Illinois, Urbana, IL 61801.

[‡] Department of Chemistry.

[§] Department of Applied Physics.

^{*} Department of Inorganic Chemistry.

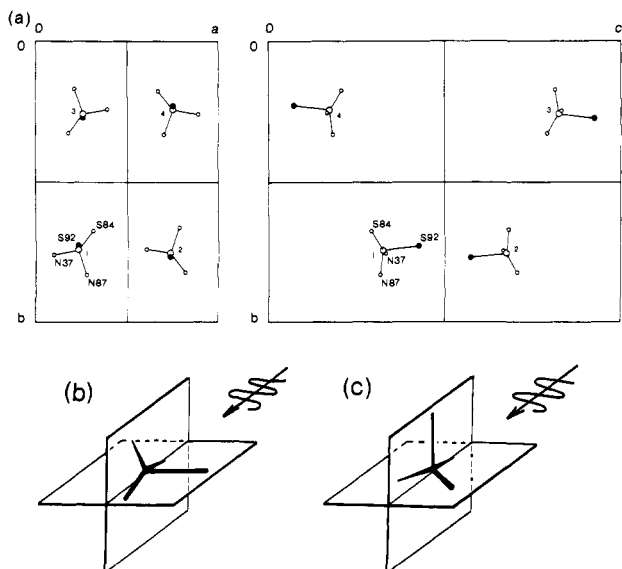


Figure 1. (a) Projections of the unit cell of poplar plastocyanin (left) on the ab plane (c axis points away from reader) and (right) on the bc plane (a points toward the reader). The Cu sites of the four symmetry-related molecules are shown enlarged by a factor of 2. N37 = N of His-37, S84 = S of Cys-84, N87 = N of His-87, S92 = S of Met-92. The coordinates of the symmetry-related molecules, indicated by small numerals, are (1) x, y, z ; (2) $1/2 + x, 1/2 - y, 1 - z$; (3) $1/2 - x, 1 - y, 1/2 + z$; (4) $1 - x, 1/2 + y, 1/2 - z$. (b) Schematic diagram of copper site in plastocyanin oriented with Cu-S(Met) vector parallel to polarization vector of plane-polarized synchrotron radiation. The crystal ab plane is then perpendicular to the polarization vector. In this orientation the contribution of S(Met) to the EXAFS should be optimized in relation to the other ligands. (c) Schematic diagram as in (b) but with Cu-S(Met) perpendicular to the polarization vector. The incident-beam propagation direction and the polarization vector are now in the ab plane of the crystal.

polarization vector and the absorber-scatterer vector (as discussed later). Hence, it is possible to maximize or minimize the contribution of the S(Met) ligand to the EXAFS by varying the orientation of a plastocyanin crystal with respect to the polarization vector of the incident X-ray beam (Figure 1). Such polarization effects can lead to dramatic differences between the EXAFS contributions from particular ligands as a function of the angles between the metal-ligand bonds and polarization vector, as has previously been observed in studies of single crystals of MoO_2S_2 .⁹

Experimental Section

X-ray Absorption Measurements. X-ray absorption spectra were measured at the Stanford Synchrotron Radiation Laboratory (SSRL) on beam line II-2 by using a Si[220] double-crystal monochromator. The storage ring was operating at 3.0 GeV with an average current of 60–70 mA. The data were recorded at room temperature as fluorescence excitation spectra by using an array of 18 NaI scintillation detectors directed at the crystal.¹⁰

To ensure accurate calibration of the X-ray photon energy, we employed internal calibrations, recording a high-resolution edge of a known standard (copper foil) simultaneously with each scan. In this procedure an ion chamber, a copper foil, and another ion chamber are placed behind the crystal. The addition of the copper foil and the final ion chamber is a general method for measuring the absorption spectrum of a standard at the same time that fluorescence (or transmission) X-ray absorption data are being collected on the sample. This internal calibration procedure allows the calibration of the energy scale to an accuracy of ± 0.1 eV.

Approximately 20 scans were averaged to give each of the EXAFS spectra reported in this paper. Each scan required approximately 20 min to record, giving a total irradiation time of less than 10 h per crystal. The programs and methods used for averaging, background removal, Fourier transformation, and curve fitting have been described previously in detail.¹¹

Crystal Characteristics and Manipulation. Plastocyanin was purified and crystallized by vapor diffusion against 2.6 M ammonium sulfate (0.1 M sodium phosphate buffer) at pH 6.0 as previously described.¹² The crystals used in these experiments were large but not entirely regular, with some well-developed faces. Edge dimensions were typically between 0.5 and 1.5 mm. The data cited here were recorded from two crystals ("crystal 2" and "crystal 7") which had dimensions $1.4 \times 0.9 \times 0.4$ mm and $1.1 \times 0.8 \times 0.5$ mm, respectively. The largest dimension in each case was parallel to a , and the other two dimensions represented vertical separations between opposite faces of the form (011). Data were also recorded from a third crystal ("crystal 6") that had a volume approximately one-third as large as the volumes of the other two crystals.

The crystal specimens were mounted in glass capillaries (wall thickness 0.01 mm, internal diameter 2 mm) or in a thin-walled rectangular Lucite cell (wall thickness ca. 0.2 mm). Over the 9.0–9.7-keV range (the Cu EXAFS region), the glass capillaries were found to contribute slightly less background absorption than the Lucite cell. Crystals 6 and 7 were mounted in glass capillaries; crystal 2 was mounted in the Lucite cell. Each capillary or cell contained a drop of mother liquor in addition to (but not in contact with) the crystal. Soft dental wax was used to seal the capillaries. The mounted specimens were supported on a Lucite two-circle goniometer that permitted rotation through ca. 120° about the incident beam direction (χ axis), rotation through 360° about an axis perpendicular to this direction (ϕ axis), and translation along the ϕ axis. The incident beam was collimated by using tantalum slits. The crystal χ axis was brought into coincidence with the collimated beam through a vertical adjustment of the entire goniometer. Approximate centering of each spectrum onto the ϕ rotation axis was achieved by viewing the specimen through a low-power stereomicroscope. The beam size was sufficiently large that the entire crystal was bathed in X-rays for all values of χ and ϕ .

The directions of the crystallographic axes discussed in this paper were initially inferred from the X-ray absorption spectra and were confirmed from X-ray precession photographs after the X-ray absorption studies were completed. The precession photographs, recorded with a conventional X-ray source, extended to a resolution of at least 2.0 Å. Thus, they not only confirmed the identification of the axes but also provided evidence that the crystals had not suffered significant radiation-induced decomposition. Verification of the lack of radiation damage is essential since a number of other Cu(II) proteins (e.g., cytochrome c oxidase) have been suggested to undergo photoreduction under the conditions of EXAFS measurements.¹³ Photoreduction is improbable in the case of copper(II) plastocyanin since the crystallographic study of copper(I) plastocyanin was at one time hampered by the tendency of the crystals to undergo photooxidation.³ In the present work, one of the first scans for each crystal was repeated at the end of the data recording period. In no case was there a detectable change in the X-ray absorption edge region or in the EXAFS. This is consistent with previous experience in recording diffraction data for plastocyanin crystals with synchrotron radiation at the DORIS storage ring in Hamburg. During diffraction data collection, the crystals still diffracted strongly at angles corresponding to 2-Å resolution after 24 h of continuous exposure to synchrotron radiation.³ The current EXAFS measurements at SSRL involved irradiation of each crystal for less than 10 h. The available evidence suggests that the plastocyanin crystals did not suffer significant photoreduction or other radiation-induced damage.

Crystal Orientation. In order to observe the desired orientational enhancement of the Cu-S(Met) EXAFS, it was necessary to orient the crystal with the unit-cell c axis (and therefore the Cu-S(Met) bonds) parallel to the polarization direction, p . For the orthorhombic plastocyanin crystals, this orientation is accessible when the a axis is parallel to the propagation direction, k (i.e., pointing into the radiation source). From this orientation, rotations in χ alternately align either the b axis or the c axis with p . Using the known morphology, we mounted a crystal so that its a axis was in the horizontal plane (the plane containing k and p) at $\chi = 0^\circ$. The a axis could now be oriented parallel to p or k by an appropriate rotation of ϕ . The orientation with a parallel to k should have a reduced EXAFS amplitude relative to the orientation with a parallel to p . The minimum EXAFS amplitude (observed when a is parallel to k) will be smaller for χ values that make c parallel to p and

(9) Kutzler, F. W.; Scott, R. A.; Berg, J. M.; Hodgson, K. O.; Doniach, S.; Cramer, S. P.; Chang, C. H. *J. Am. Chem. Soc.* **1981**, *103*, 6083–6088.
(10) Cramer, S. P.; Scott, R. A. *Rev. Sci. Instrum.* **1981**, *52*, 395–399.

(11) (a) Eccles, T. K. Ph.D. Thesis, Stanford University, 1977. (b) Cramer, S. P.; Hodgson, K. O.; Stiefel, E. I.; Newton, W. E. *J. Am. Chem. Soc.* **1978**, *100*, 2748–2761. (c) Scott, R. A.; Cramer, S. P.; Shaw, R. W.; Beinert, H.; Gray, H. B. *Proc. Natl. Acad. Sci. U.S.A.* **1981**, *78*, 664–667.
(12) Chapman, G. V.; Colman, P. M.; Freeman, H. C.; Guss, J. M.; Murata, M.; Norris, V. A.; Ramshaw, J. A. M.; Venkatappa, M. P. *J. Mol. Biol.* **1977**, *110*, 187–189.

(13) Chance, B.; Angiolillo, P.; Yang, E. K.; Powers, L. *FEBS Lett.* **1980**, *112*, 178–182.

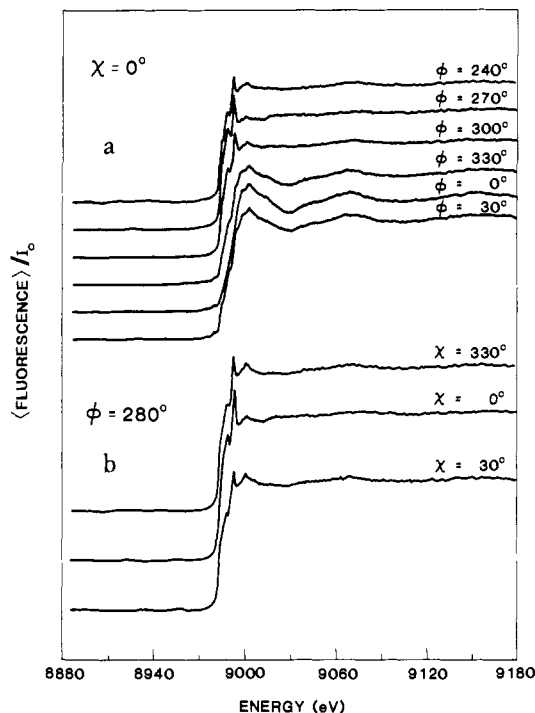


Figure 2. Changes in the X-ray absorption spectrum of a plastocyanin crystal as a function of orientation. The crystal was aligned with its *a* axis lying in the plane containing the polarization and the propagation directions. (a) Rotations in ϕ bringing the *a* axis parallel to the polarization direction ($\phi \approx 0^\circ$) or parallel to the propagation direction ($\phi \approx 270^\circ$). (b) Rotations in χ (with the *a* axis lying parallel to the propagation direction). $\chi = 0^\circ$ corresponds to the *c* axis parallel to the polarization direction.

larger for χ values that make *b* parallel to *p*. Figure 2a shows selected spectra from ϕ rotations (at $\chi = 0^\circ$) for crystal 7 with *a* in the horizontal plane. Dramatic changes in both the EXAFS and the absorption edge region are clearly visible. Particularly notable is a pre-edge spike whose intensity is inversely correlated with the amplitude of the EXAFS oscillations. The height of this spike was used to determine all orientations, since it was visibly more sensitive to orientation than were the EXAFS modulations. A maximum in the spike corresponded to a minimum in the EXAFS, which in turn indicated that *a* was parallel to *k*.

Representative absorption spectra for a series of χ orientations (with ϕ set so that *a* is parallel to *k*) are shown in Figure 2b. A minimum in the EXAFS (as determined by a maximum in the spike) occurs when the *c* axis and the Cu-S(Met) bonds are parallel to *p*. Alignment of the crystals using only the X-ray absorption effects was remarkably accurate. For example, crystal 2 was identified as having its *c* axis parallel to *p* when $\phi = -10^\circ$ and $\chi = -25^\circ$. Subsequent crystallographic identification of the crystal orientation showed that this crystal had its *c* axis, and therefore its Cu-S(Met) bonds, parallel to *p* when $\phi = -10^\circ$ and $\chi = -27^\circ$.

Results and Discussion

Analysis of Orientation-Dependent EXAFS Effects. The complete copper X-ray absorption spectra (8670–9670 eV) were recorded for two crystals (crystal 2 and crystal 7), each in two orientations. The orientations were chosen experimentally so that one of them maximized and the other minimized the amplitude of the EXAFS. As discussed above, in these orientations the *b* and *c* axes, respectively, were close to the polarization direction. The resulting EXAFS spectra, obtained after averaging and background subtraction, are shown in Figure 3. First, we note that the EXAFS effects are highly reproducible between two crystals of similar overall dimensions but different shapes. The third crystal (crystal 6), which was smaller, gave essentially the same EXAFS as crystals 2 and 7 but with a poorer signal-to-noise ratio. Second, while the amplitude of the EXAFS changes with orientation by approximately a factor of 5, the frequency and phase of the EXAFS remain essentially the same for all orientations. This indicates that the distance to the backscattering atoms (and the identity of these atoms) is virtually the same in both

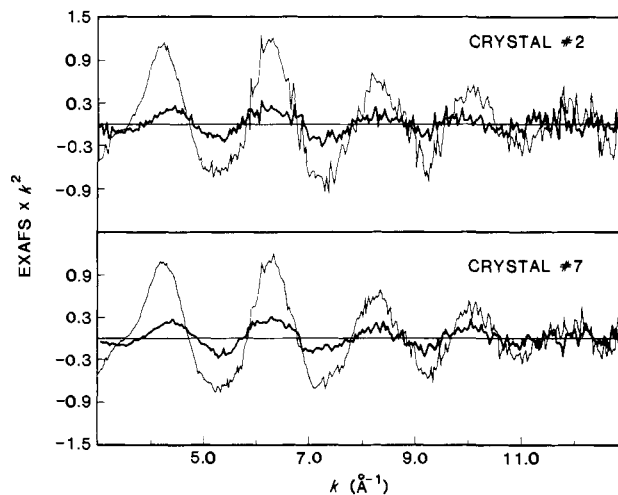


Figure 3. EXAFS spectra for two plastocyanin crystals, each in the two orientations that respectively maximize (dark line) or minimize (light line) the components of the Cu-S(Met) bonds in the direction of the X-ray polarization direction.

orientations—only the magnitudes of the atoms' contributions change.

A number of previous studies have examined the angular dependence of the EXAFS from oriented samples.^{9,14} Theoretically, the EXAFS contribution from a single scatterer is equal to the matrix element $\langle f\hat{e}\cdot\hat{r}|i\rangle^2$ where $|i\rangle$ and $|f\rangle$ are the initial and final state of the system, respectively, and \hat{e} is the polarization vector of the radiation. The \hat{e} term may be replaced with $\cos^2\theta$ where θ is the angle between \hat{e} and \hat{r} . The matrix element is then evaluated to give the familiar EXAFS equation $\langle f\hat{r}|i\rangle^2 =$

$$\chi_{\text{EXAFS}}(k) = \frac{1}{k} \sum_s N_s \frac{|f_s(\pi, k)|}{R_{\text{as}}^2} \sin [2kR_{\text{as}} + \alpha_{\text{as}}(k)] \exp(-2\sigma_{\text{as}}^2 k^2) \exp(-\lambda/R_{\text{as}})$$

where the expression is summed over all scatterers *s*. The photoelectron wave vector, *k*, is defined by $k = (2m_e(E - E_0))^{1/2}/\hbar$ where m_e is the electron mass and E_0 is the threshold energy. N_s is the number of scatterers of the same type at a distance R_{as} from the absorbing atom. The term $|f_s(\pi, k)|$ represents the backscattering amplitude of the atoms; σ_{as}^2 is the mean-square displacement in R_{as} , λ is the photoelectron mean-free path, and $\alpha_{\text{as}}(k)$ is a *k*-dependent total phase shift in the outgoing and backscattering photoelectron waves.

For randomly oriented samples, the $\cos^2\theta$ term is averaged over all possible orientations to give a factor of $1/3$. Thus, when the current EXAFS results are compared with the expected EXAFS amplitude on the basis of randomly oriented model compounds, the amplitude must be multiplied by a factor of $3\cos^2\theta$ where θ is the angle between *p* and the absorber-scatterer vector.

In measurements on plastocyanin crystals, when the *c* axis is oriented parallel to the polarization direction, the EXAFS should be dominated by the S(Met) ($\theta = 8^\circ$) and contain only minor contributions from the other ligands ($\theta = 66\text{--}95^\circ$, mean = 82°). Quantitatively, $\chi_{\text{EXAFS},c} = 3[(\cos^2 172^\circ)S_{\text{Met}} + (\cos^2 95^\circ + \cos^2 85^\circ)N_{\text{His}} + (\cos^2 66^\circ)S_{\text{Cys}}] = 2.94S_{\text{Met}} + 0.05N_{\text{His}} + 0.50S_{\text{Cys}}$. For the orientation in which *b* is parallel to the polarization direction, the Cu-S(Cys-84) and Cu-H(His-87) bonds have significant components in the direction of the polarization, while the Cu-S(Met-92) and Cu-N(His-37) bonds are nearly perpendicular to the polarization direction. The expected EXAFS is $\chi_{\text{EXAFS},b} = 3[(\cos^2 82^\circ)S_{\text{Met}} + (\cos^2 97^\circ + \cos^2 166^\circ)N_{\text{His}} + (\cos^2 43^\circ)S_{\text{Cys}}] = 0.06S_{\text{Met}} + 2.87N_{\text{His}} + 1.60S_{\text{Cys}}$.

(14) Beni, G.; Platzman, P. M.; *Phys. Rev. B: Solid State* **1976**, *14*, 1514–1518. Heald, S. M.; Stern, E. A. *Ibid.* **1977**, *16*, 5549–5559. Heald, S. M.; Stern, E. A. *Ibid.* **1978**, *17*, 4069–4081. Cox, A. D.; Beaumont, J. H. *Philos. Mag., [Part] B* **1980**, *42*, 115–126. Templeton, D. H.; Templeton, L. K. *Acta Crystallogr. Sect. A* **1980**, *A36*, 237–241.

Table I. Results of Least-Squares Fits to EXAFS Data for Single Crystals of Poplar Plastocyanin

crystal	axis parallel to polarization	distances, Å			coordination numbers				F^a
		$R_{\text{Cu-N}}$	$R_{\text{Cu-S}}$	$R_{\text{Cu-S}'}$	N_{N}	N_{S}	$N_{\text{S}'}$	$N_{\text{N}}/N_{\text{S}}$	
2	c	2.07	2.11		0.3	0.6			0.90
		2.06	2.11	2.79	0.3	0.6	0.2		0.90
	b	2.01	2.06		5.2	1.8			1.31
		2.01	2.06	2.72	5.0	1.8	0.3		1.29
7	c	2.01	2.09		0.8	0.5			0.64
		2.01	2.09	2.74	0.8	0.5	0.2		0.62
	b	1.98	2.09		3.5	1.4			0.99
		1.98	2.09	2.72	3.6	1.4	0.4		0.95
6	b	1.96	2.08		3.6	0.7			1.54
		1.96	2.08	2.80	3.6	0.8	0.2		1.53
average	c	2.04	2.10	2.76	0.6	0.6		1	
	b	1.98	2.08	2.73	4.1	1.3		3	
values of R from crystal structure ^{3,4} calculated ^b	c	2.04, 2.10			2.13	2.90			
	b				0.05	0.50	2.95	0.10	
					2.87	1.60	0.06	1.80	

^a F is a goodness-of-fit criterion defined by $F = [\sum k^6 (\text{data-fit})^2 / (\text{no. of points})]^{1/2}$ where the sum is over all points. ^b See text for calculation of the expected EXAFS amplitudes for the two orientations.

EXAFS spectra are functions of energy (i.e., they are plotted in frequency space). A physically more meaningful presentation is obtained upon Fourier transformation of the EXAFS.¹⁵ This procedure gives the radial distribution function around the absorbing copper atom. Fourier transforms of the EXAFS spectra in Figure 3 were computed over a k range of 4–12 Å⁻¹ with k^3 weighting and are shown in Figure 4. While the transforms from different orientations and from different crystals are similar in shape, they clearly reflect the orientational dependence of the EXAFS amplitude. The noise levels are indicated by the magnitude of the peaks in the transforms at R greater than 4 Å. Only the major peak at 1.6–1.7 Å in each transform is unequivocally above the noise level. This peak corresponds to ligand atoms at ca. 2 Å from the Cu, after a correction is made for the phase shift.^{11a} Contributions to this peak are therefore made by the histidine nitrogens and the cysteine sulfur. There is no obvious contribution from the fourth ligand, the methionine sulfur, at 2.9 Å. The transforms strongly resemble those recorded previously for solutions of plastocyanin⁷ and azurin.⁸ The complete lack of any peak above 2 Å in the transforms provides very strong evidence against any Cu–S(Met) contribution to the EXAFS. In particular, the transform amplitude in this region is no larger for the orientation with c parallel to p than for the orientation with b parallel to p , even though the latter orientation can contain only negligible Cu–S(Met) EXAFS.

Fourier transforms are useful for visualizing the qualitative features of the EXAFS. Quantitation is most readily achieved by least-squares optimization of a function that models the expected EXAFS. The variables in the fitting procedure are the numbers of scatterers and their distances from the absorber. Details of the least-squares calculations have been given previously.¹¹ The amplitudes and phases for the curve-fitting may be either calculated ab initio or derived empirically from model compounds with known structures. In this study we have utilized the empirical curve-fitting procedures that were applied to previous studies of the solution EXAFS of blue copper proteins.

The high-frequency noise in the EXAFS data may be removed by backtransforming only the physically significant portion of the Fourier transforms (Fourier filtering). The Fourier-filtering process used a square window extending from approximately 1 to 4 Å with the sides of the window function smoothed by multiplication with a half-Gaussian of width of 0.3 Å. Models were fitted to the unfiltered data, the smoothed data (where the noise was removed by Fourier filtering), and the first-shell data (where the main transform peak was isolated by Fourier filtering). No significant differences between the different fits were observed.

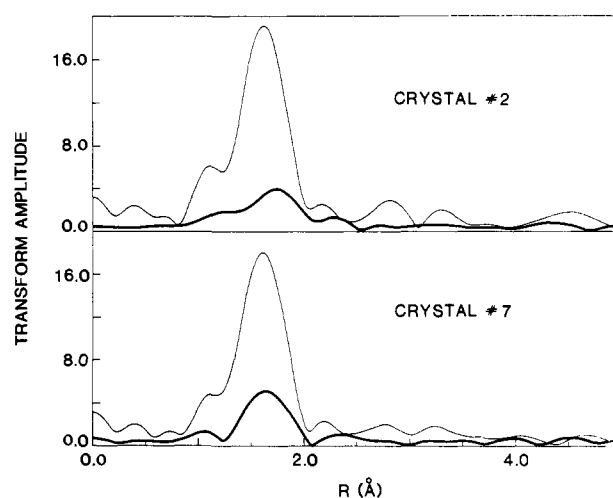


Figure 4. Fourier transforms of the EXAFS spectra shown in Figure 3 over a k range of 4–12 Å⁻¹. The major peak in each transform contains the contributions of the N(His) and S(Cys) atoms. The transforms of the EXAFS data from the orientation with the maximum contribution from the Cu–S(Met) EXAFS (c in the parallel direction) (dark line) are lower in amplitude and show no feature that can be attributed to the S(Met) atom.

Table I contains a summary of the best fits for the *unfiltered* data by using initially two shells (N and S) and then three shells (N, S, and S'). The numbers and distances of the atoms in the first shell (N and S) and the quality of the fit were insensitive to the addition of the distant shell (S'). The best fit to the data for crystal 2 with b parallel to the polarization direction is typical and is shown in Figure 5.

Several conclusions can be drawn from the data in Table I. First, the copper–ligand distances determined for the three close ligands are in good agreement both with those determined by X-ray diffraction^{3,4} and with those determined by solution EXAFS studies.⁷ Second, the observed numbers of close nitrogen and sulfur ligands (N_{N} and N_{S}) and the ratio of these numbers ($N_{\text{N}}/N_{\text{S}}$) are in qualitative agreement with the expected values for the two different orientations. The differences between the observed and calculated values are somewhat larger than the estimated fitting error of ± 0.5 atoms. However, this error estimate is likely to be low since it does not include allowances for the strong dependence of apparent number on crystal orientation and the less-than-complete polarization of the X-ray beam. Third, there is no evidence that the fourth and most distant ligand, S(Met), contributes significantly to the EXAFS in either orientation. When included in the fit, this sulfur atom refines to approximately the

(15) Sayers, D. E.; Stern, E. A.; Lytle, F. W. *Phys. Rev. Lett.* 1971, 27, 1204–1207.

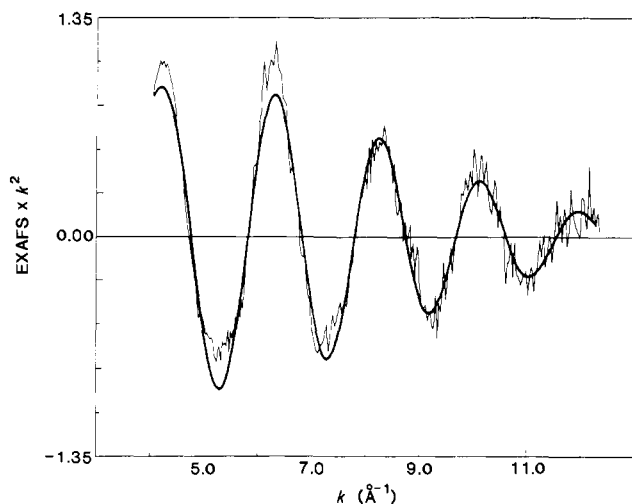


Figure 5. The best fit to the data for crystal 2 oriented with b parallel to the polarization direction. The light line is the unfiltered data; the dark line is the least-squares fit to the data by using Cu-N and Cu-S shells. The parameters derived from the fit are discussed in the text.

same low occupancy (0.2–0.3) at the same distance from the Cu atom (2.7–2.8 Å, shorter than the 2.9 Å found in the crystal structure) for both orientations. This short apparent distance could possibly be explained by an anharmonic Cu-S potential.¹⁶ However, the addition of a wave representing the S(Met) at a long distance results in an insignificant improvement in the quality of the fit, and, as suggested by the appearance of the Fourier transforms, improves the fit as much for the orientation with b parallel to p as it does for the orientation with c parallel to p . For both orientations we believe that the improvement in the fit is solely due to an increase in the number of degrees of freedom of the system and not due to the S(Met) EXAFS. Finally, the present results for the orientation with b in the polarization direction allow us to quantify the noise level in the data. The peak in the transform at approximately 2.2 Å could potentially be ascribed to Cu-S(Met) EXAFS were it not for the fact that the amplitude of this peak is independent of orientation. The orientational invariance of this peak suggests that it is due to experimental noise. The opportunity to compare the two orientations is thus an important advance over the previous solution studies.

The complete absence of EXAFS oscillations attributable to the S(Met) ligand is surprising. Klein and co-workers¹⁷ have reported the absence of EXAFS modulations attributable to nearest-neighbor atoms in a series of oxo-bridged manganese dimers. This observation was attributed to the static disorder of the nearest-neighbor atoms, in which a heterogeneity of absorber-scatterer distances resulted in destructive interference of the EXAFS modulations and hence the absence of the expected EXAFS. Conceivably, destructive interference between the Cu-S(Met) EXAFS and the Cu-(imidazole carbon) EXAFS could account for the lack of Cu-S(Met) EXAFS for solutions of plastocyanin. Application of the "group fitting" procedure to the solution EXAFS of plastocyanin suggests that such interference is not occurring.¹⁸ The single-crystal EXAFS of plastocyanin provides confirmation that static disorder is not responsible for the lack of Cu-S(Met) EXAFS since such interference would depend strongly on crystal orientation. The plastocyanin single-crystal EXAFS would be expected to show C(imidazole) EXAFS in the orientation with b parallel to p and Cu-S(Met) EXAFS in the orientation with c parallel to p . The peak at 2.7 Å in the b parallel to p orientation is fit with 5–6 carbons at ~3.0 Å. No such features are observed for c parallel to p (see Figure 4).

(16) Eisenberger, P.; Brown, G. S. *Solid State Commun.* **1979**, *29*, 481–484.

(17) Kirby, J. A.; Robertson, A. S.; Smith, J. P.; Thompson, A. C.; Cooper, S. R.; Klein, M. P. *J. Am. Chem. Soc.* **1981**, *103*, 5529–5537.

(18) Tullius, T. D.; Co, M. S.; Hodgson, K. O., unpublished results.

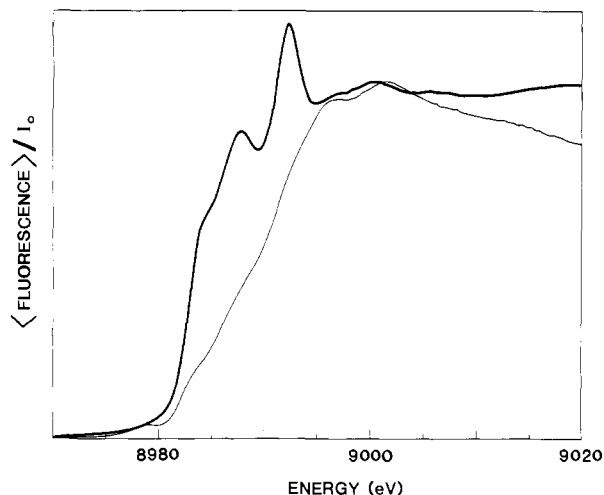


Figure 6. Comparison of X-ray absorption edge regions for the two orientations of a plastocyanin crystal described in the caption to Figure 3. The dark line corresponds to the orientation in which the Cu-S(Met) bonds lie parallel to the X-ray polarization direction. The light line is the spectrum obtained with b parallel to the polarization direction.

An alternate mechanism for reducing EXAFS amplitudes involves *dynamic* disorder. Reduction in the EXAFS amplitude for atoms having large Debye-Waller factors is a well-known phenomenon. The plastocyanin crystal structure, however, gives no indication of an anomalously large temperature factor for the S(Met) atom.³ A possible explanation of this apparent discrepancy is that the EXAFS amplitude is sensitive to the *relative* motion of a pair of atoms about their mean *separation*, while crystallographic temperature factors depend on the motions of individual atoms about their mean *positions*. When two atoms are strongly bonded, their motions are generally highly correlated, and the mean vibrational deviation from their internuclear distance is smaller than it would be for uncorrelated motions.¹⁹ On the other hand, if a backscattering atom and an X-ray absorbing atom are bonded weakly or not at all, then their motions are largely uncorrelated, and the backscatterer makes a correspondingly small contribution to the EXAFS. For example, the EXAFS of copper(II) sulfate pentahydrate does not have contributions from the second-nearest-neighbor oxygen atoms at 2.4 Å.¹⁹ This result has been attributed to the essentially uncorrelated motion of the Cu and O atoms. It is possible that a similar explanation accounts for the lack of Cu-S(Met) EXAFS in plastocyanin, in which case the Cu-S(Met) bond is shown to be very weak.

Orientation Effects in X-ray Absorption Edges. In contrast with the absence of any spectacular orientational dependence for the frequencies in the EXAFS, the absorption edges of plastocyanin change remarkably as a function of crystal orientation (Figure 6). Because synchrotron radiation is plane polarized, the transitions excited by the radiation are orientationally selected. This effect is dramatically illustrated by a sharp transition around 8992 eV and by a weak transition near 8978 eV. The former (the "spike" of Figure 2) is seen only when the Cu-S(Met) bonds are parallel to the X-ray polarization direction and the latter only when the Cu-S(Met) bonds are perpendicular to this direction.

We are currently unable to assign most of the observed transitions in the absorption-edge region. An exception is the lowest energy transition near 8978 eV. This is clearly the $1s \rightarrow 3d$ transition commonly seen in other Cu(II) complexes.²⁰ The fact that it occurs here is consistent with a recent assignment in which the $3d_{x^2-y^2}$ orbital is perpendicular to the Cu-S(Met) bond and is the site of the vacancy in the 3d shell of the Cu atom in copper(II)-plastocyanin.⁶ The symmetry-forbidden $1s \rightarrow 3d$ transition (into the $3d_{x^2-y^2}$ orbital) becomes somewhat allowed under the reduced-site symmetry and is seen only when the polarization

(19) Joyner, R. W. *Chem. Phys. Lett.* **1980**, *72*, 162–164.

(20) Hu, V. W.; Chan, S. I.; Brown, G. S. *Proc. Natl. Acad. Sci. U.S.A.* **1977**, *74*, 3821–25.

direction does not lie in a nodal plane of the $3d_{x^2-y^2}$ orbital. SCF X_α calculations have been successful in assigning the edge transitions for single crystals of $\text{MoO}_2\text{S}_2^{2-}$.^{9,21} We are in the process of extending such calculations to the blue copper site of plastocyanin.

Conclusions

Measurements of the X-ray absorption spectra of plastocyanin crystals in two orientations have enabled us to demonstrate the lack of any EXAFS oscillations attributable to the S(Met) ligand at 2.9 Å from the copper atom and to discover orientation-dependent X-ray absorption edge effects. A possible explanation of the absence of EXAFS oscillations caused by the S(Met) atom is that the motions of the copper and the S(Met) are essentially uncorrelated. Uncorrelated motions, if substantiated, may be taken as an operational definition of nonbonding in cases where crystallographically determined interatomic distances do not lead to an unequivocal description. EXAFS investigation of model compounds with long copper-sulfur bonds could help to determine the generality of this observation. The dichroic absorption edges suggest a location for the Cu $3d_{x^2-y^2}$ orbital that is consistent with a recent redetermination of the electronic structure of the blue copper site.⁶

The failure of EXAFS measurements to detect the presence of an important ligand atom is significant as it demonstrates the risks of using EXAFS as a tool for investigating metal sites in

metalloproteins ab initio. However, the present work demonstrates that EXAFS in combination with crystal structure analysis may reveal new details of the bonding in metal coordination environments. Single-crystal EXAFS in particular is shown to provide significant structural information beyond that normally obtained in solution EXAFS experiments.

Acknowledgment. This work was supported by grants from the National Science Foundation (PCM 79-04915), the Australian Research Grants Committee (C 80-15377), and Esso Australia Ltd. and a University of Sydney Research Travel Grant. J.E.H. is the recipient of a National Science Foundation Predoctoral Fellowship, and R.A.S. was supported by a National Institutes of Health Postdoctoral Fellowship (5 F32 HL06047). Synchrotron radiation beam time and some of the equipment and resources used in this study were provided by the Stanford Synchrotron Radiation Laboratory with the financial support of the National Science Foundation (under Contract DMR 77-27489) in cooperation with the Department of Energy and by the National Institutes of Health SSRL Biotechnology Resource (RR 01749). The assistance of Dr. M. Murata and V. A. Norris in the preparation of the plastocyanin specimens is gratefully acknowledged.

Registry No. Plastocyanin, 9014-09-9.

Supplementary Material Available: Tables representing the averaged X-ray absorption data recorded from crystal 2 and crystal 7 in the *b* parallel to the polarization and *c* parallel to the polarization orientations have been deposited as Table II (9 pages). Ordering information is given on any current masthead page.

(21) (a) Kutzler, F. W. Ph.D. Thesis, Stanford University, 1981. (b) Kutzler, F. W.; Natoli, C. R.; Misemer, D. K.; Doniach, S.; Hodgson, K. O. *J. Chem. Phys.* 1980, 73, 3274-3288.

Chloropalladation of Alkyl-Substituted Methylene-cyclopropanes

Thomas A. Albright,^{*1a,d} Paula R. Clemens,^{1b} Russell P. Hughes,^{*1b,c} Donald E. Hunton,^{1b} and Lawrence D. Margerum^{1b}

Contribution from the Departments of Chemistry, University of Houston, Houston, Texas 77004, and Dartmouth College, Hanover, New Hampshire 03755. Received November 23, 1981

Abstract: The chloropalladation reactions of methylene-cyclopropanes bearing alkyl substituents at the three-membered ring are shown to involve 1,3 addition of the elements of Pd-Cl to the organic molecule, with cleavage of the 2,3 σ bond of the ring. Isopropylidene-cyclopropane is inert toward chloropalladation, in contrast to 2,2-dimethylmethylene-cyclopropane, which gives a 9:1 mixture of **13** and **14**. The *cis* and *trans* isomers of 2,3-dimethylmethylene-cyclopropane give an identical chloropalladation product, **16**, which exists as a mixture of two diastereoisomeric pairs of enantiomers in a solvent-dependent ratio. The apparent lack of selectivity in the latter reaction is shown to be due to rapid η^3 to η^1 to η^3 transformations of the organic ligand after the chloropalladation step. The true stereochemistry of 1,3 chloropalladation is revealed in the reactions of *cis*-9-methylenebicyclo[6.1.0]nonane (**19**) to give only **20** and of *trans*-9-methylenebicyclo[6.1.0]nonane (**21**) to give a 4:1 mixture of **22** and **23**. Formation of these products is rationalized in terms of suprafacial addition of the elements of Pd-Cl to a ring that is opening stereospecifically in a disrotatory mode, with the breaking bond bending away from the metal. *cis*-7-Methylenebicyclo[4.1.0]heptane (**17**) affords **18** in a reaction that involves suprafacial addition of Pd-Cl while the ring opens disrotatorily with the breaking bond bending toward the metal, followed by a rapid η^3 to η^1 to η^3 isomerization of the kinetic product **25**. The absence of η^3 to η^1 to η^3 interconversions of **20**, **22**, and **23** is rationalized in terms of steric blocking by the nine-membered rings; no such impediment exists for **18**. Monomeric acetylacetonato (acac) derivatives of **16**, **18**, **20**, and **22** are described. Theoretical calculations at the extended Hückel level indicate that the two disrotatory modes of ring cleavage require similar activation energies for a model methylene-cyclopropane-PdCl₂(NCH) complex. The disrotatory motion of the carbon-carbon bond breaking away from the metal is very slightly favored on electronic grounds. On the other hand, the conrotatory route has a much higher activation energy associated with it. The reaction is, technically, symmetry allowed. The HOMO-LUMO crossing is only weakly avoided, and a small HOMO-LUMO gap is obtained at the transition state. Therefore, the conrotatory path exhibits behavior akin to that in symmetry-forbidden reactions. At some stage in the ring opening, the Cl transfer from Pd to the organic ligand begins. There is a strong interaction between the filled Cl lone-pair orbital and the LUMO of the complex that is concentrated on the two noncoordinated methylene carbons. The Cl transfer should require little, if any, additional activation energy.

The organometallic chemistry of highly strained organic rings has been a topic of considerable interest over the past decade,

particularly with regard to the role of transition-metal compounds in the cleavage of carbon-carbon bonds. The transition-metal